ELSEVIER

Journal of Organometallic Chemistry 490 (1995) 1–6

Journal of Organometallic Chemistry

The coordinatively unsaturated cluster cations $[Pt_3\{M(CO)_3\}(\mu\text{-}Ph_2PCH_2PPh_2)_3]^+$ (M = Re, Mn)

Jianliang Xiao, Eva Kristof, Jagadese J. Vittal, Richard J. Puddephatt *

Department of Chemistry, University of Western Ontario, London N6A 5B7, Canada

Received 4 May 1994; in revised form 15 August 1994

Abstract

The coordinatively unsaturated cluster $[Pt_3(\mu_3\text{-}CO)(\mu\text{-}dppm)_3]^{2+}$ (**1**, dppm = $Ph_2PCH_2PPh_2$) reacts with $Na^+[M(CO)_5]^-$ to give the mixed metal clusters $[Pt_3\{M(CO)_3\}(\mu\text{-}dppm)_3]^+$ (M = Re, **2**; Mn, **3**). The new clusters are characterized by spectroscopic methods and, for M = Re, by an X-ray structure determination. The Pt_3Re core in **2** is tetrahedral with particularly short metal–metal distances.

Keywords: Platinum; Manganese; Rhenium; Metal clusters; Carbonyl; Diphosphine

1. Introduction

Heteronuclear cluster compounds of the transition metals are of continuing interest in part because of their relationship with bimetallic alloy catalysts [1,2]. Of particular interest are Pt–Re cluster complexes because of the importance of bimetallic $Pt/Re/Al_2O_3$ catalysts in reforming of petroleum [3]. However, there are still relatively few Pt–Re clusters compared, for example, with mixed-metal platinum clusters containing ruthenium and osmium [1e,4]. More work in this area is clearly justified.

It has been shown that the coordinatively unsaturated cluster $[Pt_3(\mu_3\text{-}CO)(\mu\text{-}dppm)_3]^{2+}$ (**1**, dppm = $Ph_2PCH_2PPh_2$) can mimic many properties of a platinum surface [5], so it was considered that related coordinatively unsaturated Pt–Re cluster compounds might provide some insight into the structure and reactivity of the Pt-Re surface. This work reports the synthesis of the clusters $[Pt_3\{M(CO)_3\}(\mu\text{-}dppm)_3]^+$ (M = Re, **2**; Mn, **3**) and the structure of the Pt_3Re complex. A preliminary account of part of this work has been published [6].

2. Results and discussion

Compounds **2** and **3** were obtained in good yields by reacting the parent cluster **1** with $[M(CO)_5]^-$ (M = Re and Mn) according to Eq. (1). Both complexes **2** and **3** were dark red in colour and are decomposed slowly by air.

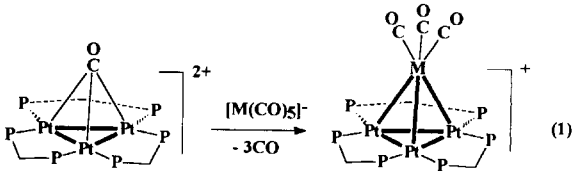

(1)

The spectroscopic parameters of **2** and **3** are similar, and will be discussed together. In the ^{31}P NMR spectra, both compounds displayed a singlet with complex satellites resulting from coupling to ^{195}Pt that are typical of $Pt_3(\mu\text{-}dppm)_3$ complexes with C_3 symmetry [7]. In particular, the observation of long-range coupling $^2J(PtP)$ and $^3J(PP)$ for these species is indicative of the presence of metal–metal bonded, P–Pt–Pt–P units, with the range of Pt–Pt–P bond angles of 147–159°, through which effective transmission of coupling information through the metal–metal bond occurs [8]. The IR spectrum of each compound contained three CO-

* Corresponding author.

SSDI 0022-328X(95)05180-1

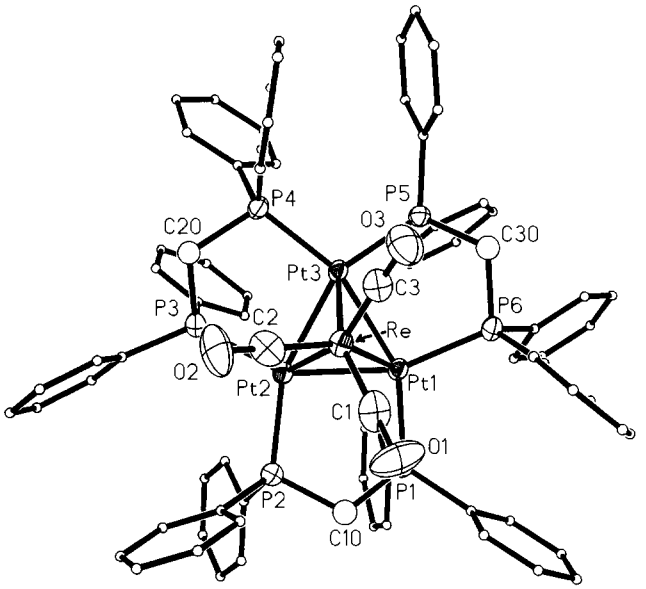

Fig. 1. A top view of the structure of the cluster cation **2**. Phenyl carbon atoms are shown as spheres of arbitrary radius.

stretching bands, ranging from 1981–1825 cm^{-1}. In addition, the products of reaction of $[Pt_3(\mu_3\text{-}CO)(\mu\text{-}dppm)_3]^{2+}$ and of the ^{13}CO-substituted cluster $[Pt_3(\mu_3\text{-}^{13}CO)(\mu\text{-}dppm)_3]^{2+}$ with $[Re(CO)_5]^-$ gave identical IR spectra, indicating that the bridging carbonyl ligand in **1** had been replaced during the reaction. Together these observations indicate that compounds **2** and **3** have a similar tetrahedral structure, with the triangular platinum face being capped by rhenium and manganese carbonyl fragments.

The structure of **2** as the $[BPh_4]$ salt has been confirmed by X-ray diffraction. A view of the cluster cation is shown in Fig. 1. The complex adopts a tetrahedral geometry, consisting of a triangular arrangement of platinum atoms, with one face of the Pt_3 triangle capped by a $Re(CO)_3$ group. A related compound is $[Pt_3\{\mu_3\text{-}SnMe_2(PO_2F_2)\}(\mu\text{-}dppm)_3]^+$, in which the capping CO ligand in **1** is replaced by a μ_3-$SnMe_2(PO_2F_2)$ group [7]. As with other related complexes [5], each edge of the Pt_3 triangle is bridged by a μ-dppm group, and the Pt–P distances are normal. The stereochemistry of the rhenium centre may be considered to be pseudo-octahedral with $Re(CO)_3Pt_3$ coordination. However, as shown in Fig. 1, the geometry is distorted towards trigonal prismatic because the $Re(CO)_3$ unit is twisted so that the carbonyl ligands are directed towards P(1), P(3) and P(5) and away from P(2), P(4) and P(6). The distortion probably arises as a result of steric effects. The $Re(CO)_3$ group is relatively bulky and occupies a cavity defined by the phenyl substituents of the dppm ligands. Each Pt_2P_2C unit adopts an envelope conformation with the CH_2 group of the dppm ligand at the "flap" position. All CH_2 groups are directed towards the $Re(CO)_3$ side of the $Pt_3(dppm)_3$ unit. In this conformation, all phenyl substituents on the $Re(CO)_3$ side are equatorial and all phenyl groups on the other side are axial. This leads to a much larger cavity on the $Re(CO)_3$ side. In addition, the phosphorus atoms P(1), P(3) and P(5) are displaced out of the Pt_3 plane away from the rhenium fragment by 0.455(3)–0.476(3) Å while P(2), P(4) and P(6) lie approximately in this plane. As a result, the cavities are asymmetric and the $Re(CO)_3$ twist leads to lower steric hindrance. This effect is easily understood by viewing the space-filling diagrams shown in Fig. 2.

The incorporation of the $Re(CO)_3$ group causes a significant decrease in the Pt–Pt bonding distances compared to the precursor **1**. While the Pt–Pt distances in **1** range from 2.613(1)–2.650(1) Å, which correspond to normal single Pt–Pt bonds [5], those in **2** [2.5930(9)–2.6114(7) Å] are the shortest among **1** and its derivatives. Like the Pt–Pt separations, the Pt–Re distances in **2** [2.649(1)–2.685(1) Å] also appear to be the shortest known. In previously reported Pt–Re compounds, the Pt–Re distances have been found in the range 2.71–2.91 Å, with almost half having values from 2.83–2.87 Å [4]. Typical examples may be found in compounds such as $[PtRe_2(CO)_{12}]$ which has a Pt–Re bond length of 2.8309(5) Å [9], and $[PtRe_4(CO)_{17}]^{2-}$ where the average Pt–Re distance is 2.750 Å [4b]. Therefore both the Pt–Pt and the Pt–Re bonds in **2** are presumably strong. It is interesting to note that the Pt–Sn distances in the 42-electron cluster $[Pt_3\{\mu_3\text{-}SnMe_2(PO_2F_2)\}(\mu\text{-}dppm)_3]^+$ are shorter than those found in related compounds containing *trans* capping ligands, such as the 44-electron complex $[Pt_3(\mu_3\text{-}CO)(\mu_3\text{-}SnF_3)(\mu\text{-}dppm)_3]^+$ [7]. It has been suggested that in such compounds the *trans* influence of ligands across the Pt_3 triangle leads to a mutual bond weakening [7,10]. Since neither $[Pt_3\{\mu_3\text{-}SnMe_2(PO_2F_2)\}(\mu\text{-}dppm)_3]^+$ nor **2** has a capping ligand *trans* to tin or rhenium respectively, the Pt–Sn or Pt–Re bonds are expected to be strong. Complex **2** is the first example in which a rhenium fragment caps a triangular platinum face. Such a structure may well exist in the Pt–Re ensembles at heterogeneous Pt–Re catalyst surfaces [3] and, if so, a strong binding interaction may be predicted.

The cluster cation **2** has a valence electron count of only 54, whereas most tetrahedral clusters, in which each metal center has the 18-electron count, have a total of 60 valence electrons [11]. Hence the cluster is coordinatively unsaturated. If it is assumed that each platinum center has a 16-electron count while the rhenium center has an 18-electron count, the metal–metal bonding is most easily rationalized in terms of the following model. It is already known that the three filled M–M bonding orbitals of a planar $Pt_3(\mu\text{-}dppm)_3$ fragment have $a_1' + e'$ symmetry, and that a pyramidal $Re(CO)_3^+$ fragment has three vacant acceptor orbitals

which have $a_1 + e$ symmetry [12]. Clearly then, three donor–acceptor metal–metal bonds are possible in which the M–M bonding orbitals of the $Pt_3(\mu\text{-dppm})_3$ fragment are the donors and the $Re(CO)_3^+$ fragment orbitals are the acceptors as depicted in **4**. In this way,

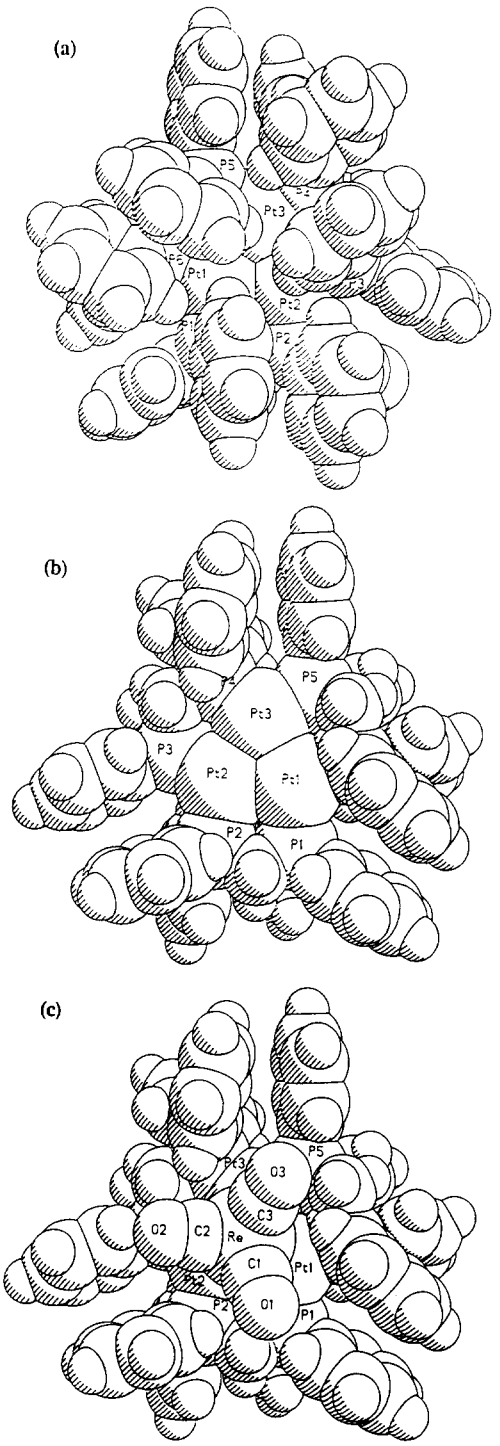

Fig. 2. Space-filling diagrams showing the different cavity sizes on either side of the Pt_3 triangle: (a) the bottom face with axial phenyl groups leaving a very small cavity; (b) the top face with equatorial phenyl groups leaving a large but unsymmetrical cavity; (c) the position of the $Re(CO)_3$ unit within this cavity.

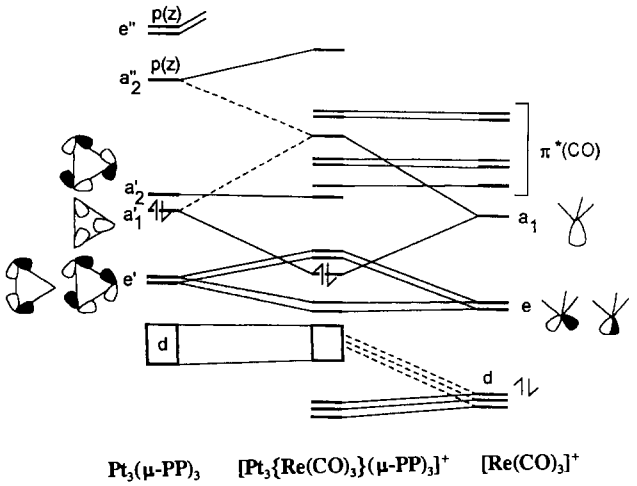

Fig. 3. Energy correlation diagram for interaction of the $Pt_3(\mu\text{-dppm})_3$ and $Re(CO)_3^+$ fragments. The top three occupied MO's are the $a_1 + e$ metal–metal bonding MOs.

each Pt atom naturally shares 16 valence electrons, and the Re atom shares 18 valence electrons. In the MO treatment, the fragment orbitals combine to form bonding and antibonding MOs each with $a_1 + e$ symmetry, and there are six cluster electrons which just fill the bonding MO's as shown in Fig. 3 [12]. Strong Pt–Re bonding is expected, consistent with the observation of short Pt–Re bonds. However, this type of three-centre two-electron bonding is not usually very strong, and it is not clear why the metal–metal bonds are among the shortest known.

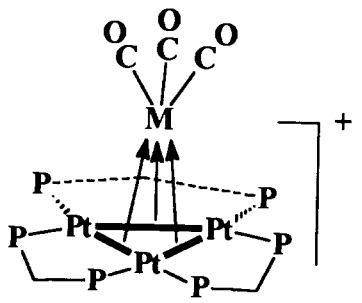

4

Both complexes **2** and **3** decompose slowly in the air. The Pt_3Re cluster reacted, even in the solid state, with dioxygen to give the dioxo cluster, $[Pt_3\{Re(CO)_3\}(\mu_3\text{-}O)_2(\mu\text{-dppm})_3]^+$ but the products of reaction of **3** with O_2 have not been characterized [6]. The $M(CO)_3$ unit is displaced more easily from **3** than from **2**, probably because of the Pt–Mn bond being weaker than the Pt–Re bond. For example, in refluxing CH_2Cl_2 solution the Pt_3Mn cluster **3** was fragmented and converted to the known compound [13,14], $[Pt_3(\mu_3\text{-Cl})(\mu_3\text{-CO})(\mu\text{-dppm})_3]^+$, whereas **2** was stable under these conditions. Both **2** and **3** decomposed in solution in CH_2Cl_2 in the presence of CO to give $[Pt_3(\mu_3\text{-Cl})(\mu_3\text{-}$

$CO)(\mu\text{-dppm})_3]^+$, but the reaction was much faster in the case of **3**.

There is an isolobal analogy between the fragment $[Pt_3(\mu\text{-dppm})_3]$ and $[C_5H_5]^-$ such that the cation **2** may be considered isolobal to neutral $[(C_5H_5)Re(CO)_3]$. Similarly, the anionic $[(C_5H_5)M(CO)_3]^-$ should be isolobal to neutral $[Pt_3\{M(CO)_3\}(\mu\text{-dppm})_3]$ with M = Cr, Mo or W, and $[(C_5H_5)M(CO)_2]^-$ should be isolobal to $[Pt_3\{M(CO)_2\}(\mu\text{-dppm})_3]$ with M = Fe, Ru or Os. In view of the evidence for strong M–M bonding in **2**, attempts have been made to prepare these complexes, but so far without success. The only promising reaction was that of **1** with $[HM(CO)_4]^-$ or $[M(CO)_4]^{2-}$ when M = Fe [15]. This gave a single complex, but it had low thermal stability and could only be characterized by spectroscopic methods. In CH_2Cl_2 solution, it was quantitatively converted to $[Pt_3(\mu_3\text{-}Cl)(\mu_3\text{-}CO)(\mu\text{-dppm})_3]^+$ by reaction with the solvent in a period of hours at room temperature by displacement of the carbonyliron fragment [13]. The reaction was much faster than the analogous reaction of **3** described above.

3. Experimental details

Reactions were carried out under an atmosphere of dinitrogen using standard Schlenk techniques. The compounds $[Pt_3(\mu_3\text{-}CO)(\mu\text{-dppm})_3][PF_6]_2$ [16] $NaRe(CO)_5$ [17] and $LiMn(CO)_5$ [18] were prepared by the literature procedures. IR spectra were recorded with a Perkin-Elmer 2000 FTIR spectrometer, and the NMR spectra were recorded by using a Varian Gemini-300 with chemical shifts being referenced to TMS (^1H) and 85% H_3PO_4 ($^{31}P\{^1H\}$). Elemental analyses were performed by Galbraith Laboratories, Inc.

3.1. $[Pt_3\{Re(CO)_3\}(\mu\text{-dppm})_3][PF_6].CH_2Cl_2$ (2[PF_6])

To a suspension of **1** (411 mg, 0.20 mmol) in THF (35 ml) was added $NaRe(CO)_5$ (0.24 mmol) in THF (8.5 ml), resulting in an immediate colour change to dark brown. After stirring overnight, the solution was concentrated to about 3 ml and then diethyl ether (20 ml) was layered on the top of the solution. Compound **2[PF_6]** was precipitated as black-red crystalline solid. Solvent was then removed, the solid was washed with distilled water and finally dried in vacuum. Yield: 85%. Anal. Calc. for $C_{79}H_{68}Cl_2F_6O_3P_7Pt_3Re$: C, 42.38; H, 3.07. Found: C, 42.63; H, 3.15%. IR (Nujol): $\nu(CO)/cm^{-1}$ = 1981s, 1882sh, 1871s. NMR (CD_2Cl_2): $\delta(^1H)$ = 4.19 [m, CH_2]; $\delta(^{31}P)$ = 7.9 [s, $^1J(PtP)$ = 2411 Hz, $^2J(PtP)$ = 248 Hz, $^3J(PP)$ = 198 Hz].

Once formed, compound **2[PF_6]** can be handled in the air for a short time only because a reaction occurs, even in the solid state, over a period of days. Compound **2[PF_6]** can be recrystallized from CH_2Cl_2/diethyl ether or CH_2Cl_2/hexane, but the crystals were not of X-ray quality.

3.2. $[Pt_3\{Re(CO)_3\}(\mu\text{-dppm})_3][BPh_4].CH_2Cl_2$ (2[BPh_4])

To a solution of **2[PF_6]** (44 mg) in MeOH (10 ml) was slowly added $NaBPh_4$ (102 mg, 15-fold excess) in MeOH (5 ml), immediately resulting in the precipitation of a crystalline solid. After stirring for 30 min, solvent was removed and the product was washed with MeOH. Yield: 90%. Compound **2[BPh_4]** was recrystallized as black plates from CH_2Cl_2/diethyl ether. Anal. Calc. for $C_{103}H_{88}BCl_2O_3P_6Pt_3Re$: C, 51.27; H, 3.68. Found: C, 51.31; H, 3.55%. IR (Nujol): $\nu(CO)/cm^{-1}$ = 1979s, 1873sh, 1867s. NMR (CD_2Cl_2): $\delta(^1H)$ = 4.18 [m, CH_2]; $\delta(^{31}P)$ = 8.0 [s, dppm] with the same coupling constants as found for **2[PF_6]**.

3.3. $[Pt_3\{Mn(CO)_3\}(\mu\text{-dppm})_3][PF_6].CH_2Cl_2$ (3[PF_6])

The compound was prepared in a manner similar to that for **2[PF_6]**, except that $LiMn(CO)_5$ was used. Compound **3[PF_6]** was isolated in 70% yield, and was recrystallized from CH_2Cl_2/diethyl ether. Anal. Calc. for $C_{79}H_{68}Cl_2F_6MnO_3P_7Pt_3$: C, 45.02; H, 3.26. Found: C, 44.80; H, 3.43%. IR (Nujol): $\nu(CO)/cm^{-1}$ = 1975s, 1903 m, 1825 m. NMR (CD_2Cl_2): $\delta(^1H)$ = 4.49[m, CH_2]; $\delta(^{31}P)$ = −5.4 [s, $^1J(PtP)$ = 3030 Hz, $^2J(PtP)$ = 170 Hz, $^3J(PP)$ = 160 Hz].

3.4. Complex 1 with $K[FeH(CO)_4]$ or $Na_2Fe(CO)_4$

These reactions were carried out in a similar way to that described above, but the product, which had identical spectra for both reactions, was not sufficiently stable to be recrystallized. IR(Nujol): $\nu(CO)$ cm^{-1} = 1992s, 1928s. NMR (CD_2Cl_2): $\delta(^1H)$ = 4.05, 5.90 [m, CH_2P_2]; $\delta(^{31}P)$ = −9.6[s, br, $^1J(PtP)$ = 3097 Hz, dppm].

3.5. X-ray crystal structure analysis of $[Pt_3\{Re(CO)_3\}(\mu\text{-dppm})_3][BPh_4].CH_2Cl_2$(2[$BPh_4$].$CH_2Cl_2$)

Single crystals of **2[BPh_4].CH_2Cl_2** were grown by diffusion of diethyl ether into a solution of the compound in CH_2Cl_2. A crystal of suitable size (0.12 × 0.14 × 0.30 mm) was obtained by cutting a long rod-like crystal along the (0, −2, −1) plane and was coated with apiezon grease to prevent solvent loss. The data collection was carried out on an Enraf-Nonius CAD4F diffractometer using graphite monochromated Mo Kα radiation [19] at −50°C (to prevent solvent loss). Least-squares fits of 21 accurately cantered reflections ($24.1 \leq 2\theta \leq 32.1°$) gave cell constants and an orientation matrix. The Niggli matrix suggested the triclinic

system. Intensity data were recorded in ω mode, at variable scan speeds and a scan width of $0.80 + 0.35\tan\theta$ with a maximum time per datum of 45 s. Background measurements were made by extending the scan by 25% on each side. Three standard reflections were monitored every 180 min of X-ray exposure time. In all, 13261 reflections in the 2θ range 0–46° and 47 repetitions of the standards were recorded.

The NRCVAX crystal structure programs was used for data processing and least-squares refinements [20]. The data were corrected for Gaussian absorption and gave maximum and minimum transmission factors of 0.575 and 0.458. The space group *P*-1 was assumed. The equivalent reflections were averaged ($R_{int} = 0.012$) leaving 12550 independent reflections. The structure was solved by using the SHELXS-86 program [21] and subsequent difference Fourier techniques. Anisotropic thermal parameters were assigned for the Pt, Re, P, O and C atoms of the carbonyl groups and were refined. One molecule of dichloromethane solvent was located in the difference Fourier routines. Two different orientations were seen for the phenyl ring with carbon atoms C(211) to C(216) and were related by a rotation (of 56.4(7)°) along the axis containing C(211) and C(216) atoms. The two disordered rings were refined in the least-squares cycles with occupancy factors of 0.5/0.5. The hydrogen atoms were placed in ideal positions (C–H = 1.08 Å) and their thermal parameters were assigned as 10% greater than for the attached carbon

Table 1
Selected bond distances (Å) and angles (deg) for $[Pt_3\{Re(CO)_3\}(\mu\text{-dppm})_3][BPh_4]\cdot CH_2Cl_2$ (2[BPh_4])

Pt(1)–Pt(2)	2.6114(7)	Pt(1)–Pt(3)	2.5930(9)
Pt(2)–Pt(3)	2.6078(9)	Pt(1)–Re	2.6839(7)
Pt(2)–Re	2.6488(8)	Pt(3)–Re	2.6850(8)
Pt(1)–P(1)	2.287(3)	Pt(1)–P(6)	2.288(3)
Pt(2)–P(2)	2.291(3)	Pt(2)–P(3)	2.293(3)
Pt(3)–P(4)	2.279(3)	Pt(3)–P(5)	2.285(3)
Re–C(1)	1.85(1)	Re–C(2)	1.88(1)
Re–C(3)	1.85(1)	C(1)–O(1)	1.18(1)
C(2)–O(2)	1.16(1)	C(3)–O(3)	1.19(1)
Pt(2)–Pt(1)–Pt(3)	60.14(2)	Pt(2)–Pt(1)–Re	60.01(2)
Pt(2)–Pt(1)–P(1)	92.27(7)	Pt(2)–Pt(1)–P(6)	158.12(8)
Pt(3)–Pt(1)–Re	61.14(2)	Pt(3)–Pt(1)–P(1)	150.14(7)
Pt(3)–Pt(1)–P(6)	98.07(8)	Re–Pt(1)–P(1)	117.03(7)
Re–Pt(1)–P(6)	109.49(7)	P(1)–Pt(1)–P(6)	109.5(1)
Pt(1)–Pt(2)–Pt(3)	59.58(2)	Pt(1)–Pt(2)–Re	61.35(2)
Pt(1)–Pt(2)–P(2)	98.01(7)	Pt(1)–Pt(2)–P(3)	147.94(7)
Pt(3)–Pt(2)–Re	61.43(2)	Pt(3)–Pt(2)–P(2)	157.59(7)
Pt(3)–Pt(2)–P(3)	90.36(8)	Re–Pt(2)–P(2)	109.83(8)
Re–Pt(2)–P(3)	116.22(8)	P(2)–Pt(2)–P(3)	111.5(1)
Pt(1)–Pt(3)–Pt(2)	60.28(2)	Pt(1)–Pt(3)–Re	61.10(2)
Pt(1)–Pt(3)–P(4)	159.46(8)	Pt(1)–Pt(3)–P(5)	91.49(7)
Pt(2)–Pt(3)–Re	60.04(2)	Pt(2)–Pt(3)–P(4)	99.20(8)
Pt(2)–Pt(3)–P(5)	149.73(7)	Re–Pt(3)–P(4)	109.37(7)
Re–Pt(3)–P(5)	118.01(7)	P(4)–Pt(3)–P(5)	108.8(1)
Pt(1)–Re–Pt(2)	58.64(2)	Pt(1)–Re–Pt(3)	57.76(2)
Pt(1)–Re–C(1)	95.6(4)	Pt(1)–Re–C(2)	150.1(3)
Pt(1)–Re–C(3)	118.6(3)	Pt(2)–Re–Pt(3)	58.53(2)
Pt(2)–Re–C(1)	115.6(4)	Pt(2)–Re–C(2)	93.0(3)
Pt(2)–Re–C(3)	154.2(3)	Pt(3)–Re–C(1)	152.6(4)
Pt(3)–Re–C(2)	117.9(4)	Pt(3)–Re–C(3)	97.3(3)
C(1)–Re–C(2)	88.2(5)	C(1)–Re–C(3)	90.0(5)
C(2)–Re–C(3)	91.0(5)	Re–C(1)–O(1)	175(1)
Re–C(2)–O(2)	174(1)	Re–C(3)–O(3)	176.5(9)
P(1)–C(10)–P(2)	111.2(5)	P(3)–C(20)–P(4)	109.2(5)
P(5)–C(30)–P(6)	108.6(5)		

Table 2
Crystal data for $[Pt_3\{Re(CO)_3\}(\mu\text{-dppm})_3][BPh_4]\cdot CH_2Cl_2$ (2[BPh_4])

Empirical formula	$C_{103}H_{88}B_1Cl_2O_3P_6Pt_3Re$
*f*w	2412.84
Space group	*P*-1
Cell parameters	
a	21.278(3) Å
b	19.021(5) Å
c	11.352(2) Å
α	90.10(2)°
β	99.83(1)°
γ	94.31(2)°
V	4514(2) Å^3
Z	2
ρ, g cm^{-3}: obs, calc.	1.75(5), 1.775
Temperature	−50°C
Radiation	Mo–Kα
Wavelength	0.71073 Å
Abs coeff	59.24 cm^{-1}
No. of observ.,	8885($I \geq 2.5\sigma(I)$)
Variables	392
R, R_w [a]	0.037, 0.030

[a] $R = \Sigma(\|F_o\| - \|F_c\|)/\Sigma|F_o|$;
$R_w = [\Sigma w(\|F_o\| - \|F_c\|)^2/\Sigma w|F_o|]^{1/2}$.

Table 3
Selected positional parameters and thermal parameters for 2[BPh_4] [a]

Atom	*x*	*y*	*z*	B_{iso}
Pt(1)	0.20121(2)	0.74084(2)	0.40456(4)	1.88(2)
Pt(2)	0.32388(2)	0.73424(2)	0.47675(4)	1.89(2)
Pt(3)	0.27508(2)	0.85601(2)	0.44733(4)	1.79(2)
Re	0.28367(2)	0.77623(3)	0.25621(4)	2.28(2)
P(1)	0.1805(1)	0.6232(2)	0.4354(3)	2.3(1)
P(2)	0.3255(1)	0.6139(2)	0.4789(3)	2.6(1)
P(3)	0.4186(1)	0.7884(2)	0.5736(2)	2.2(1)
P(4)	0.3664(1)	0.9281(2)	0.4967(2)	2.1(1)
P(5)	0.1890(1)	0.9221(1)	0.4369(2)	2.0(1)
P(6)	0.1070(1)	0.7909(2)	0.3414(2)	2.2(1)
C(1)	0.2533(6)	0.7052(7)	0.1451(9)	3.8(7)
C(2)	0.3646(6)	0.7720(7)	0.2125(9)	3.4(6)
C(3)	0.2622(5)	0.8430(6)	0.1410(9)	2.9(6)
O(1)	0.2325(5)	0.6567(5)	0.0810(8)	7.1(6)
O(2)	0.4169(4)	0.7703(5)	0.1958(8)	6.1(6)
O(3)	0.2462(4)	0.8872(5)	0.0705(7)	5.1(5)
C(10)	0.2471(5)	0.5726(5)	0.4044(9)	2.5(2)
C(20)	0.4368(4)	0.8743(5)	0.5058(8)	2.0(2)
C(30)	0.1242(5)	0.8861(5)	0.3151(8)	2.3(2)

[a] All the parameters were assigned anisotropic thermal parameters given as the isotropic equivalent displacement parameter. B_{iso} is the mean of the principal axes of the thermal ellipsoid.

atoms. The hydrogen atoms were not included for the disordered phenyl rings.

In the final cycles, the refinement of 392 parameters and 8885 ($I \geq 2.5\sigma(I)$) observations, the model converged at $R = 0.037$, $R_w = 0.030$. In the final difference Fourier synthesis the electron density ranged from 1.11 to -1.11 e Å^{-3}. The top four peaks had electron densities greater than 1.0 e Å^{-3}, of which the top peak was associated with Cl(2) at a distance of 0.20 Å and the other three were associated with Re, Pt(2) and Pt(1) atoms at distances of 1.08, 1.06 and 1.04 Å respectively.

Selected bond distances and angles are listed in Table 1. The crystal data and experimental conditions are summarized in Table 2. Selected positional and thermal parameters are given in Table 3. Complete data have been deposited with the Cambridge Crystallographic Data Centre.

Acknowledgments

We thank the NSERC (Canada) for financial support, and Dr. N.C. Payne for access to X-ray facilities.

References and notes

[1] For examples see (a) R.D. Adams and W. Wu, *Organometallics*, *12* (1993) 1238, 1248; (b) M.R. Churchill, C.H. Lake, F.J. Safarowic, D.S. Parfitt, L.R. Nevinger and J.B. Keister, *Organometallics*, *12* (1993) 671; (c) L.C. Song, J.Y. Shen, Q.M. Hu, R.J. Wang and H.G. Wang, *Organometallics, 12* (1993) 408; (d) R.D. Adams, Z. Li, P. Swepston, W. Wu and J. Yamamoto, *J. Am. Chem. Soc.*, *114* (1992) 10657; (e) L.J. Farrugia, *Adv. Organomet. Chem.*, *31* (1990) 301.

[2] R.D. Adams and W.A. Herrmann, *Polyhedron*, *7* (1988) 2255–2464.

[3] J. Biswas, G.M. Bickle, P.G. Gray, D.D. Do and J. Barbier, *Catal. Rev. Sci. Eng.*, *30* (1988) 161.

[4] (a) J. Xiao, J.J. Vittal and R.J. Puddephatt, *J. Chem. Soc., Chem. Commun.*, (1993) 167; (b) T. Beringhelli, A. Ceriotti, G. Ciani, G. D'Alfonso, L. Garlaschelli, R.D. Pergola, M. Moret and A. Sironi, *J. Chem. Soc., Dalton Trans.*, (1993) 199; (c) P. Antognazza, T. Beringhelli, G. D'Alfonso, A. Minoja, G. Ciani, M. Moret and A. Sironi, *Organometallics*, *11* (1992) 1777; (d) J. Powell, J.C. Brewer, G. Gulia and J.F. Sawyer, *J. Chem. Soc., Dalton Trans.*, (1992) 2503; (e) T. Beringhelli, G. D'Alfonso and A.P. Minoja, *Organometallics*, *10* (1991) 394; (f) G. Ciani, M. Moret, A. Sironi, P. Antognazza, T. Beringhelli, G. D'Alfonso, R.D. Pergola and A. Minoja, *J. Chem. Soc., Chem. Commun.*, (1991) 1255; (g) G. Ciani, M. Moret, A. Sironi, T. Beringhelli, G. D'Alfonso and R.D. Pergola, *J. Chem. Soc., Chem. Commun.*, (1990) 1668; (h) T. Beringhelli, A. Ceriotti, G. D'Alfonso and R.D. Pergola, *Organometallics*, *9* (1990) 1053, and references therein. The Cambridge Structure Database yielded references to 15 structures containing Pt–Re bonds.

[5] R.J. Puddephatt, Lj. Manojlović-Muir and K.W. Muir, *Polyhedron*, *9* (1990) 2767.

[6] J. Xiao, J.J. Vittal, R.J. Puddephatt, Lj. Manojlović-Muir and K.W. Muir, *J. Am. Chem. Soc.*, *115* (1993) 7882.

[7] M.C. Jennings, G. Schoettel, S. Roy, R.J. Puddephatt, G. Douglas, Lj. Manojlović-Muir and K.W. Muir, *Organometallics*, *10* (1991) 580.

[8] (a) M. Rashidi and R.J. Puddephatt, *J. Am. Chem. Soc.*, *108* (1986) 7111; (b) S.S.M. Ling, N. Hadj-Bagheri, Lj. Manojlović-Muir, K.W. Muir and R.J. Puddephatt, *Inorg. Chem.*, *26* (1987) 231.

[9] M.A. Urbancic, S.R. Wilson and J.R. Shapley, *Inorg. Chem.*, *23* (1984) 2954.

[10] B.R. Lloyd and R.J. Puddephatt, *J. Am. Chem. Soc.*, *107* (1985) 7785.

[11] D.M.P. Mingos and A.S. May, in D.F. Shriver, H.D. Kaesz and R.D. Adams (eds.), The Chemistry of Metal Cluster Complexes, VCH, New York, 1990. The most common electron count for tetrahedral clusters is 60, such as in $[Ir_4(CO)_{12}]$.

[12] For previous theoretical work on Pt_3L_6 clusters and on $M(CO)_3$ fragments, see (a) D.G. Evans, *J. Organomet. Chem.*, *352* (1988) 397; (b) T.A. Albright, J.K. Burdett and M-H. Whangbo, *Orbital Interactions in Chemistry*, Wiley, New York, 1985, ch. 20.

[13] Lj. Manojlović-Muir, K.W. Muir, B.R. Lloyd and R.J. Puddephatt, *J. Chem. Soc., Chem. Commun.*, (1985) 536.

[14] M.C. Jennings, N.C. Payne and R.J. Puddephatt, *Inorg. Chem.*, *26* (1987) 3776.

[15] J.J. Brunet, F.B. Kindela and D. Neibecker, *Inorg. Synth.*, *29* (1992) 151.

[16] G. Ferguson, B.R. Lloyd and R.J. Puddephatt, *Organometallics*, *5* (1986) 344.

[17] K.P. Darst, C.M. Lukehart, L.T. Warfield and J.V. Zeile, *Inorg. Synth.*, *28* (1990) 201.

[18] J.A. Gladysz, G.M. Williams, W. Tam and D.L. Johnson, *J. Organomet. Chem.*, *140* (1977) C1.

[19] *CAD4 Diffractometer Manual* Enraf-Nonius, Delft, The Netherlands, 1988.

[20] E.J. Gabe, Y. Le Page, J-P. Charland and F.C. Lee, *J. Appl. Cryst.*, *22* (1989) 384.

[21] G.M. Sheldrick, SHELXS-86. *Structure Solving Program*, University of Gottingen, Germany, 1986.